Role of Cu Film Texture in Grain Growth Correlated to Twin Boundary Formation

Kazuyuki Kohama[a,*], Kazuhiro Ito[a], Takuya Matsumoto[a], Yasuharu Shirai[a], and Masanori Murakami[b]

[a]*Department of Materials Science and Engineering, Kyoto University, Yoshida-Honmachi, Sakyo-ku, Kyoto 606-8501, Japan*

[b]*The Ritsumeikan Trust, Nakagyo-ku, Kyoto 604-8520, Japan*

Corresponding Author: Kazuyuki Kohama

TEL: +81-75-753-5482 / FAX: +81-75-753-3579

[*]E-mail address: k.kohama@eng.mbox.media.kyoto-u.ac.jp

ABSTRACT

To understand the role of Cu film texture in grain growth at room temperature (RT) in relation to twin boundary formation, Cu films were deposited on various barrier materials, and Cu film texture was investigated by X-ray diffraction. The Cu grain growth was rapid on the barrierless SiO_2/Si substrate, and very slow on the Ta barrier due to strong (111) texture. The growth rate and the average grain diameter after keeping at RT up to ~60 days were maximized at the $(200)_{Cu}$ peak to $(222)_{Cu}$ peak area ratio of ~1.0, where the {111}, {100}, and {511} grains coexisted. Such coexistence of three or more orientations of grains is essential for facilitating Cu grain growth at RT. Similarly, average twin boundary (TB) density was maximized when Cu grain growth was facilitated. The TB formation in nano-sized Cu grains was not controlled by grain size, but caused by grain growth. The TBs could be annealing twins caused by irregularities in stacking sequence during relatively fast grain growth. The Cu film texture is concluded to be determined at the early beginning of deposition, and wettability of various barrier materials to the Cu films plays a key role in determining the film texture.

Keywords: thin films; sputtering; texture; abnormal grain growth; twinning

1. Introduction

As the widths of Cu wires reduce to a deep sub-micron scale in ultra-large scale integrated (ULSI) devices, a large resistance-capacitance delay is becoming a critical material-related issue [1]. One of the primary factors for the increase in electrical resistivity of the Cu wires is the existence of fine Cu grains. Thus, understanding the mechanism of grain growth in Cu films is essential for reducing the resistivity increase. In the past two decades there have been many investigations on grain growth in Cu thin films, and both Cu grain growth and Cu texture were reported to be affected by diffusion-barrier materials [2-10]: Strong (111) texture was observed in Cu films deposited on barriers such as Ta and Ti; in contrast, some (100)-oriented grains in addition to (111)-oriented grains were observed in Cu films on W and barrierless SiO_2. The strong (111) texture suppressed Cu grain growth and that containing (100)-oriented grains among the (111) grains facilitated Cu grain growth.

On the other hand, many twin boundaries (TBs) were observed in Cu films. TBs with nano-sized spaces inside Cu grains are known to increase mechanical strength without ductility degradation, and to have little increasing effect on resistivity [11, 12]. Since TBs are homogeneous, electrical resistivities of TBs are about one order of magnitude lower than those of high-angle grain boundaries [13]. TBs are also expected to increase electro-migration (EM) resistance when not oriented in parallel to Cu interconnects [14, 15]. Thus, TBs are believed to be useful for nano-sized Cu interconnects in ULSI devices. However, TBs are known to form easily in Cu grains not only in films, but in bulk due to their relatively low stacking fault energy. There are three possible types of TB formation: growth twins [11, 12, 16, 17], annealing twins [18-21], and deformation twins [22-25]. Growth twins and annealing twins easily

formed when deposition rates of Cu films and/or growth rates of Cu grains were fast (i.e., TB formation is the result of irregularities in stacking sequence). Furthermore, TBs of the growth twins are usually oriented in parallel to a film surface, and thus they are expected not to be useful for enhancing EM resistance. Hence, we focused on annealing twins, which we assumed probably correlates with the grain growth mentioned above.

In this study, Cu films were deposited on various barrier materials, and Cu film texture was investigated by X-ray diffraction (XRD). The texture was evaluated by the area ratio of a $(200)_{Cu}$ peak to a $(222)_{Cu}$ peak. To elucidate the degree to which Cu growth is facilitated in a specific range of the ratio, Cu grain growth was traced as a function of time kept at room temperature (RT) and was systematically characterized by the ratio. The Cu grain growth was represented by resistivity decrease in the Cu films. Simultaneously, to make correlation between the TB formation and the Cu grain growth clear, the TBs were observed in Cu films by scanning ion microscopy (SIM) and transmission electron microscopy (TEM) after keeping at RT. Finally, to explain Cu film texture variation with barrier materials, the wettability of various barrier films to deposited Cu films about 10 nm in thickness and the textures of the films were investigated.

2. Experimental Procedure

About 250 nm-thick Cu-film deposition followed various types of barrier deposition on SiO_2/Si substrates in a radio frequency magnetron sputter system. Barrier samples were a 150 nm-thick Ta or TaN layer, layers composed of 75 nm-thick Ta and 75 nm-thick TaN as Ta/TaN or TaN/Ta, a 100 nm-thick Ti or TiN layer, and 50 nm-thick Ti and TiN as Ti/TiN or TiN/Ti. The Cu films were also deposited on barrierless substrates

of SiO_2/Si and $(11\bar{2}0)$-oriented sapphire. Prior to film deposition, the substrates were ultrasonically cleaned with acetone and isopropyl alcohol. Additionally, the sapphire substrate was cleaned with buffered hydrofluoric acid. The base pressure prior to deposition was approximately 1×10^{-6} Pa. The sputtering power was kept at 300 W. The working pressure for pure metal (Cu, Ta, Ti) deposition and for metal nitride (TaN, TiN) deposition was about 1 Pa and 0.5 Pa, respectively. Ar gas and Ar/N_2 mixed gases were used for the pure metal depositions and for the metal nitride depositions, respectively. The substrate holder was placed 100 mm above the target. The purity of the Cu, Ta, and Ti targets was 99.99 %.

The resistivity and the texture of the Cu films were measured by van der Pauw method and XRD method, respectively. The (111) and (100) textures in the Cu films were evaluated by a conventional θ-2θ scan. The texture was represented by area ratio (α) of the $(200)_{Cu}$ peak to the $(222)_{Cu}$ peak in the θ-2θ spectra, which was estimated by peak fitting using two pseudo-Voigt functions corresponding to $K_{\alpha1}$ and $K_{\alpha2}$ peaks and the background [26]. The $(511)_{Cu}$ peak is out of range of 2θ in the θ-2θ scan using the Cu K_α-ray, and thus the (511) texture was evaluated by a θ scan, where 2θ was set to 50.5°, for example, as the angle corresponding with $(200)_{Cu}$, and θ was changed in the range between 0° and 50°. When [511] is perpendicular to the Cu film surface, two peaks were observed to be symmetric about 25°. Microstructures such as grain size and TBs in Cu films kept up to about 270 days at RT were observed by SIM and TEM. For plan-view TEM observation, specimens with thinned-down Ta barrier layers or Cu films were made as Cu/5 nm-thick Ta/SiO_2/Si or 20 nm-thick Cu/SiO_2/Si. Wettability of various barrier materials to the Cu films was investigated by atomic force microscope (AFM) using about 10 nm-thick Cu films.

3. Results and Discussion

3.1. Room Temperature Grain Growth Depended on Film Texture

Figures 1(a) and 1(b) show portions of XRD spectra around the $(200)_{Cu}$ and $(222)_{Cu}$ peaks in the θ-2θ scan, respectively, for the barrierless Cu/SiO_2 sample kept at RT. Both $(200)_{Cu}$ and $(222)_{Cu}$ peak areas increased with increasing keeping time. The peak areas estimated by peak fitting are depicted as a function of keeping time in Figure 1(c). The estimated values for both $(200)_{Cu}$ and $(222)_{Cu}$ peak areas increased rapidly at the beginning of grain growth, and their increases slowed down drastically after about one day. Similarly, both peak areas increased with increasing keeping time in all the samples, but the $(200)_{Cu}$ peak was not observed in the Cu/Ta and Cu/Ti samples even after keeping at RT for 150 days or more. Thus, the Cu/Ta and Cu/Ti samples had strong (111) texture.

The degree of texture of the samples was expressed by the area ratio (α) of the $(200)_{Cu}$ peak to the $(222)_{Cu}$ peak in the θ-2θ spectra, as mentioned before. The α values for six samples, Cu/Ta, Cu/Ta/TaN, Cu/sapphire, Cu/SiO_2, Cu/TaN/Ta, and Cu/TaN, are depicted as a function of the keeping time (Fig. 2). Those for the as-deposited Cu samples (left-most circles in each plot of Fig. 2) varied with the barrier materials, indicating that the Cu film texture was determined by the barrier material. The α values for the Cu/Ta/TaN, Cu/TaN/Ta, and Cu/TaN samples decreased with the keeping time, while those for the barrierless Cu/sapphire and Cu/SiO_2 samples increased with the keeping time. The α values settled to specific values after sufficient keeping time in all the samples, different values for each sample. For the Cu/Ta sample, the α value (= 0) did not change at all.

Since the peak-area increase with keeping time indicates the growth of each $(200)_{Cu}$ or $(222)_{Cu}$ grain, the resistivity measurement was the most suitable method to understand average grain growth of the samples. Resistivity increase of the present pure-Cu films was explained mainly by grain boundary scattering. Figure 3 shows resistivity for the six samples as a function of the keeping time. The resistivity of the as-deposited Cu films varied with the barrier materials, indicating the as-deposited Cu grain size was dependent on the barrier material. The resistivity decreased with the keeping time for all the samples (i.e., Cu grain growth), and the resistivity decrease for each sample showed a similar trend to the α value change (Fig. 2). Thus, the decrease in resistivity for the Cu/Ta/TaN, Cu/TaN/Ta, and Cu/TaN samples is caused mainly by (111) grain growth, and that for the barrierless Cu/sapphire and Cu/SiO_2 samples is caused by (100) grain growth. This suggests that preferential orientation of grains for growth is controlled by the barrier materials. The resistivity reached the minimum value after sufficient keeping time in all the samples, and the minimum resistivity values were different for each sample. For example, the lowest and the highest values were observed for the Cu/TaN/Ta and Cu/Ta/TaN samples, respectively.

The resistivity decrease and α value change with the keeping time showed similar trends, and this suggests that grain growth was controlled by the film texture. While slight amount of {511} grains were reported to exist in addition to {111} and {100} grains in EBSD observation of Cu films [27-30], unfortunately the $(511)_{Cu}$ peak is out of range of 2θ in the θ-2θ scan using the Cu K_α-ray, and thus the (511) texture was evaluated by θ scan, as mentioned before. Typical XRD spectra of the θ scan (2θ = 50.5°) for ten samples after keeping at RT for about 200 or more days are shown in Figure 4. The XRD spectra seemed to be divided into three groups: (i) two $(200)_{Cu}$

peaks symmetric about θ = 25° (Fig. 4(a)), (ii) three $(200)_{Cu}$ peaks consisting of two peaks symmetric about θ = 25° in addition to a peak at θ = 25° (Fig. 4(b), and (iii) a single $(200)_{Cu}$ peak at θ = 25° (Fig. 4(c)). The two peaks symmetric about θ = 25° and the peak at θ = 25° correspond to {511} and {100} grains, respectively. The figure suggests a correlation between {511} grains and {100} grains: the volume fraction of {511} grains increased with decreasing fraction of {100} grains, thereby decreasing the α value. Thus, the Cu film textures were divided into three groups, consisting of {111} and {511} mixed grains, {111}, {511}, and {100} mixed grains, and {111} and {100} mixed grains, and the Cu film texture trend can be represented by the α value. Note that {111} grains were a main component in all Cu films.

Based on these results, the relationship among resistivity, Cu film texture, and keeping time at RT was summarized in Figure 5. The vertical and horizontal axes represent the resistivity of the Cu films and the α value (i.e., Cu film texture), respectively. The keeping time change is represented by the symbol change as shown in the inset scale. The resistivity of the as-deposited Cu films, around keeping time of 30-50 minutes, varied with the α value, indicating the average grain size of as-deposited Cu films depended on the Cu film texture (i.e., barrier material), and the initial resistivity was the lowest at α ~ 0 (Cu/Ta). On the other hand, the resistivity reduction rate (i.e., grain growth rate) exhibited the maximum value at the specific α value of ~1.0 (Cu/sapphire) due to (100) abnormal grain growth. The resistivity reached the lowest value of ~2.0 μΩcm at the similar specific α value of ~1.0 (Cu/TaN/Ta) due to (111) abnormal grain growth. These observations indicate that Cu grain growth at RT was not dependent on the initial grain size, but was facilitated around the α value of ~1.0. This suggests that the driving force for the grain growth is not mainly grain boundary energy

reduction, which is the driving force for normal grain growth, but minimization of crystallographically dependent energies [31]. At the α value of ~1.0, the {111}, {100}, and {511} grains coexisted, and such coexistence of three or more orientations of grains is essential for facilitating Cu grain growth at RT rather than preference for the (111) or (100) grain growth.

3.2. Twin Boundary Formation Caused by Grain Growth

Nano-sized Cu films are known to have TBs regardless of film preparation techniques such as sputtering and electroplating. As mentioned in the Introduction, the TBs are believed to be useful for nano-sized Cu interconnects due to increase of electro-migration resistance [14, 15]. A part of TB formation is believed to be related with the grain growth [18-20], and thus SIM observation was carried out in this study to investigate TB formation during the grain growth. Figure 6 shows typical SIM plan-view images of the Cu/TaN samples after keeping at RT for 14, 51, 192, and 263 days. After 14 days, the Cu film still consisted of a large amount of fine grains and relatively small amount of coarse grains. This suggests that RT grain growth was relatively slow in this sample. As the keeping time increased, the size difference between the coarse and fine grains increased, and amounts of coarse and fine grains increased and decreased, respectively. These observations indicate that such Cu grain growth pertains particularly to abnormal grain growth. Further grain growth was not observed after 192 days, and the grain growth was believed to be saturated at the keeping time between 51 and 192 days. The tendency of the RT grain growth in the Cu/TaN sample is consistent with the resistivity reduction tendency (Fig. 5), and the resistivity reached the minimum value after about 70 days. On the other hand, TBs were

not obviously observed in the fine grains, but were observed in the coarse grains. This suggests that the TB formation in nano-sized Cu grains was caused by the grain growth.

Based on similar SIM observations for all the samples, average grain diameter and TB density were evaluated and plotted as a function of the α value in Figures 7(a) and 7(b), respectively. The average grain diameter was about 100~200 nm over a wide range of α values, and found to be maximized at about 500 nm in a narrow range with the α value of ~1.0 (Fig. 7(a)). This is consistent with the minimum resistivity in a similar α range (Fig. 5). Similar trend was found in the relation between the average TB density and the α value (Fig. 7(b)), and the TB density was maximized at ~4.6 x 10^6 m^{-1} at the α value of ~1.0. This suggests that the TB density increased with increasing average grain diameter, and thus the average number of TBs in a grain was plotted as a function of average grain diameter in Fig. 8. The average number of TBs in a grain was estimated by the product of the average TB density and the average grain diameter. A linear relationship was obtained between these values, and the linear function intersected the horizontal axis at about 130 nm. This suggests that the TB number in a grain is proportional to grain size, and TBs might not be formed in grains smaller than a certain size (~130 nm).

To confirm grain-size dependence on the TB formation, TEM plan-view observation was carried out for the Cu/5 nm-thick Ta/SiO_2/Si and 20 nm-thick Cu/SiO_2/Si samples. A little grain growth in the Cu films on the Ta barrier due to strong (111) texture is expected to have a fine microstructure, while facilitating Cu grain growth on the barrierless SiO_2/Si substrate is expected to have relatively large grains. For easy plan-view observation, thickness of the Ta barrier in a TEM specimen was reduced to 5 nm for the Cu/5 nm-thick Ta/SiO_2/Si sample. To reduce the Cu grain size

after grain growth, the Cu film thickness was reduced by a factor of about ten for the 20 nm-thick Cu/SiO_2/Si samples. The TEM plan-view images of both samples are shown in Figures 9(a) and 9(b). The Cu/5 nm-thick Ta/SiO_2/Si sample consisted of Cu grains with average grain diameter of ~80 nm, and the Cu grain diameter was distributed in the range between ~50 nm and ~300 nm (Fig. 9(a)). Thus, there were some grains larger than 130 nm in diameter; however, TB was hardly observed in all grains regardless of diameter. In contrast, the 20 nm-thick Cu/SiO_2/Si sample consisted of relatively small grains about 50 nm in diameter (Fig. 9(b)). The TB formation was observed in some of those grains smaller than 130 nm in diameter. These TEM observation results indicate that the TB formation in nano-sized Cu grains was not controlled by grain size, but caused by grain growth. The TBs would not form in the Cu films with slow growth rate such as Cu/Ta samples due to the strong (111) texture, while TBs could form in Cu films in which grain growth facilitates. The TBs could be annealing twins caused by irregularities in stacking sequence during relatively fast grain growth. Partial dislocations in the TBs can be moved by internal stress in the grains, and such plastic deformation leads to reduction of elastic strain energy in the grains. Therefore, increasing a number of TBs with grain growth is expected to make strain energy relaxation easier.

3.3. Barrier-Material Effect on Determining Cu Film Texture (10 nm-Thick Films)

To clarify how and when the texture of the 250 nm-thick Cu films was determined, texture of the 10 nm-thick Cu films was investigated using XRD. The texture was similar to that of the 250 nm-thick Cu films (not shown). This indicates that the texture of the Cu films was not produced during grain growth, but was made at the early

beginning of deposition. Typical AFM images of the Cu films for the Cu/Ta, Cu/Ta/TaN, Cu/TaN/Ta, Cu/SiO_2, and Cu/TaN samples after keeping at RT for about 10 days are shown in Figure 10. The lateral Cu layer growth was observed in the Cu/Ta and Cu/Ta/TaN samples, while Cu agglomeration was observed in Cu/TaN/Ta, Cu/SiO_2, and Cu/TaN samples, and morphology of Cu islands became coarse as the α value became larger. This suggests that wettability of the various barriers to Cu films plays a key role in determining the texture. The good wettability made a continuous Cu film on the barrier, leading to strong (111) texture.

The (111) texture is reported to be preferential in thin Cu films, but the (100) texture becomes major in thick Cu films [8-10, 32, 33]. However, there has not been any report in which correlation between the Cu film texture and the wettability of various barrier materials was mentioned. In the present study, the texture of Cu films on various barrier materials seemed to be determined at the early beginning of deposition, and wettability of the barrier materials to the Cu films determined the texture. Thus, nucleation rates of the $(111)_{Cu}$ and $(100)_{Cu}$ grains were calculated as a function of a contact angle, based on thermodynamics during physical vapor deposition [34], and a ratio of calculated nucleation rates between $(111)_{Cu}$ and $(100)_{Cu}$ grains as a function of the contact angle is shown in Figure 11. In the calculation, surface energies (γ_v) of the $(111)_{Cu}$ and $(100)_{Cu}$ grains were, respectively, 1.952 and 2.166 J/m^2 [35], and temperature was 300 K. The chemical free-energy change per unit volume (ΔG_v) was not obvious, and in the range between -1×10^9 J/m^3 and -1×10^{10} J/m^3. The elastic strain energy introduced in the Cu films was ignored for simplicity in calculation. The nucleation rate of the $(111)_{Cu}$ grains was higher than that of the $(100)_{Cu}$ grains in the small contact angles (high wettability) in all ΔG_v. This is consistent with the

experimental results, and thus such correlation between the Cu film texture and the wettability of various barrier materials can be explained by thermodynamics during physical vapor deposition. Such Cu film texture at nucleation affects the grain growth, which follows the nucleation.

4. Conclusions

Cu grain growth at RT was not dependent on initial grain size, but was affected by Cu film texture (α value), which depended on barrier material. The Cu grain growth was rapid on the barrierless SiO_2/Si substrate, and very slow on the Ta barrier. The growth rate and the average grain diameter after keeping at RT were maximized at the α value of ~1.0. The Cu film textures were divided into three groups, consisting of {111} and {511} mixed grains, {111}, {511}, and {100} mixed grains, and {111} and {100} mixed grains, and the Cu film texture trend can be represented by the α value. The {111} grains were a main component in all Cu films. At the α value of ~1.0, the {111}, {100}, and {511} grains coexisted, and such coexistence of three or more orientations of grains is essential for facilitating Cu grain growth at RT. Similarly, average TB density was maximized at the α value of ~1.0. The relation also showed that the average number of TBs in a grain was in proportion to the average grain diameter, suggesting a critical grain size to form TBs (about 100 nm in diameter). However, the TEM observation results indicate that the TB formation in nano-sized Cu grains was not controlled by grain size, but caused by grain growth. The TBs would not form in the Cu films with slow growth rate such as Cu/Ta samples due to the strong (111) texture, while TBs could form in Cu films in which grain growth facilitates. The TBs could be annealing twins caused by irregularities in stacking sequence during relatively fast grain

growth. The Cu film texture is concluded to be determined at the early beginning of deposition, and wettability of various barrier materials to the Cu films plays a key role in determining the film texture.

Acknowledgements

This work was supported by Research Fellowships of the Japan Society for the Promotion of Science for Young Scientists (Kohama). The author (Ito) would like to thank the Research Foundation For Materials Science.

REFERENCES

[1] Bohr MT, El-Mansy YA. IEEE T Electron Dev 1998;45:620.

[2] Zielinski EM, Vinci RP, Bravman JC. J Appl Phys 1994;76:4516.

[3] Vinci RP, Bravman JC. Mater Res Soc Symp P 1993;308:337.

[4] Tracy DP, Knorr DB, Rodbell KP. J Appl Phys 1994;76:2671.

[5] Kuschke WM, Kretschmann A, Keller R-M, Vinci RP, Kaufmann C, Arzt E. J Mater Res 1998;13:2962.

[6] Cao ZH, Lu HM, Meng XK. Mater Chem Phys 2009;117:321.

[7] Ueno K, Ritzdorf T, Grace S. J Appl Phys 1999;86:4930.

[8] Pantleon K, Somers MAJ. J Appl Phys 2006;100:114319.

[9] Pantleon K, Gholinia A, Somers MAJ. Phys Status Solidi A 2008;205:275.

[10] Ying A, Witt C, Jordan-Sweet J, Rosenberg R, Noyan IC. J Appl Phys 2011;109:014907.

[11] Lu L, Shen Y, Chen X, Qian L, Lu K. Sience 2004;304:422.

[12] Shen YF, Lu L, Lu QH, Jin ZH, Lu K. Scripta Mater 2005;52:989.

[13] Sutton AP, Balluffi RW. Interfaces in Crystalline Materials Oxford: Clarendon Press; 1995.

[14] Xu D, Sriram V, Ozolins V, Yang JM, Tu KN, Stafford GR, Beauchamp C, Zienert I, Geisler H, Hofmann P, Zschech E. Microelectron Eng 2008;85:2155.

[15] Chen KC, Wu WW, Liao CN, Chen LJ, Tu KN. Science 2008;321:1066.

[16] Zhang X, Wang H, Chen XH, Lu L, Lu K, Hoagland RG, Misra A. Appl Phys Lett 2006;88:173116.

[17] Zhang X, Anderoglu O, Hoagland RG, Misra A. JOM-J Min Met Mat S 2008;60:75.

[18] Fullman RL, Fisher JC. J Appl Phys 1951;22:1250.

[19] Dash S, Brown N. Acta Metall Mater 1963;11:1067.

[20] Meyers MA, Murr LE. Acta Metall Mater 1978;26:951.

[21] Mahajan S, Pande CS, Imam MA, Rath BB. Acta Mater 1997;45:2633.

[22] Mahajan S, Chin GY. Acta Metall Mater 1973;21:1353.

[23] Liao XZ, Zhao YH, Srinivasan SG, Zhu YT, Valiev RZ, Gunderov DV. Appl Phys Lett 2004;84:592.

[24] Zhao WS, Tao NR, Guo JY, Lu QH, Lu K. Scripta Mater 2005;53:745.

[25] Yu Q, Shan ZW, Li J, Huang X, Xiao L, Sun J, Ma E. Nature 2010;463:335.

[26] Young RA. The Rietveld Method, New York: Oxford University Press; 1993.

[27] Stangl M, Fletcher A, Acker J, Wendrock H, Wetzig K. J Electron Mater 2007;36:1625.

[28] Courtas S, Gregoire M, Federspiel X, Bicais-Lepinay N, Wyon C. Microelectron Reliab 2006;46:1530.

[29] Yoda R, Nakaue A, Onishi T, Tachibana T. Kobe Steel Engineering Reports 2002;52:66 (in Japanese).

[30] Zielinski EM, Vinci RP, Bravman JC. J Electron Mater 1995;24:1485.

[31] Zielinski EM, Vinci RP, Bravman JC. Appl Phys Lett 1995;67:1078.

[32] Lee H, Wong SS, Lopatin SD. J Appl Phys 2003;93:3796.

[33] Stangl M, Liptak M, Fletcher A, Acker J, Thomas J, Wendrock H, Oswald S, Wetzig K. Microelectron Eng 2008:85;534.

[34] Ohring M. The materials science of thin films, San Diego: Academic Press; 1992

[35] Vitos L, Ruban AV, Skriver HL, Kollar J. Surf Sci 1998;411:186.

Figure legends

Fig. 1 Portions of XRD spectra around the (a) $(200)_{Cu}$ and (b) $(222)_{Cu}$ peaks in the θ-2θ scan, respectively, for the barrierless Cu/SiO_2 sample kept at RT. (c) Peak areas increased for both peaks as a function of keeping time.

Fig. 2 The α values for (a) Cu/Ta, (b) Cu/Ta/TaN, (c) Cu/sapphire, (d) Cu/SiO_2, (e) Cu/TaN/Ta, and (f) Cu/TaN samples as a function of keeping time.

Fig. 3 The resistivity of Cu films for (a) Cu/Ta, (b) Cu/Ta/TaN, (c) Cu/sapphire, (d) Cu/SiO_2, (e) Cu/TaN/Ta, and (f) Cu/TaN samples as a function of keeping time.

Fig. 4 XRD θ scan spectra for (a) Cu/Ta, Cu/Ti, and Cu/TiN/Ti, (b) Cu/Ta/TaN, Cu/Ti/TiN, Cu/sapphire, and Cu/TaN/Ta, and (c) Cu/SiO_2, Cu/TaN, and Cu/TiN samples after keeping at RT for about 200 or more days. In the θ scan, 2θ was set to 50.5°, corresponding to $(200)_{Cu}$, and θ was changed in the range between 0° and 50°. A single peak at about 25° corresponds to {100} grains, and two peaks symmetric about 25° correspond to {511} grains.

Fig. 5 Resistivity reduction with increasing keeping time plotted as a function of the α value (depending on barrier material) for six Cu samples deposited on different barrier materials. The sample types are indicated in the figure. The change of keeping time is represented by symbol change as shown in the inset scale.

Fig. 6 SIM plan-view images of the Cu/TaN sample after keeping at RT for (a) 14, (b) 51, (c) 192, and (d) 263 days.

Fig. 7 (a) Average grain diameter (D) and (b) average twin boundary density (n) plotted as a function of the α value. These data were obtained from nine Cu samples deposited on different barrier materials after grain growth settled. The α value for each sample is shown next to the sample type in (b).

Fig. 8 Average number of twin boundaries (N) in a grain plotted as a function of average grain diameter in the Cu films deposited on the different barrier materials. The N values were estimated by the product of the average twin boundary density (n) and the average grain diameter (D). Inset numbers are the α values.

Fig. 9 TEM plan-view images of the (a) Cu/5 nm-thick Ta/SiO_2/Si and (b) 20 nm-thick Cu/SiO_2/Si samples.

Fig. 10 AFM images of Cu films for (a) Cu/Ta, (b) Cu/Ta/TaN, (c) Cu/TaN/TaN, (d) Cu/SiO_2, and (e) Cu/TaN samples after keeping at RT for about 10 days.

Fig. 11 Ratio of calculated nucleation rates between $(111)_{Cu}$ and $(100)_{Cu}$ grains as a function of the contact angle (ϕ). Surface energies (γ_v) of the $(111)_{Cu}$ and $(100)_{Cu}$ grains [35], chemical free-energy change per unit volume (ΔG_v), and temperature used in the calculations are shown in the figure.

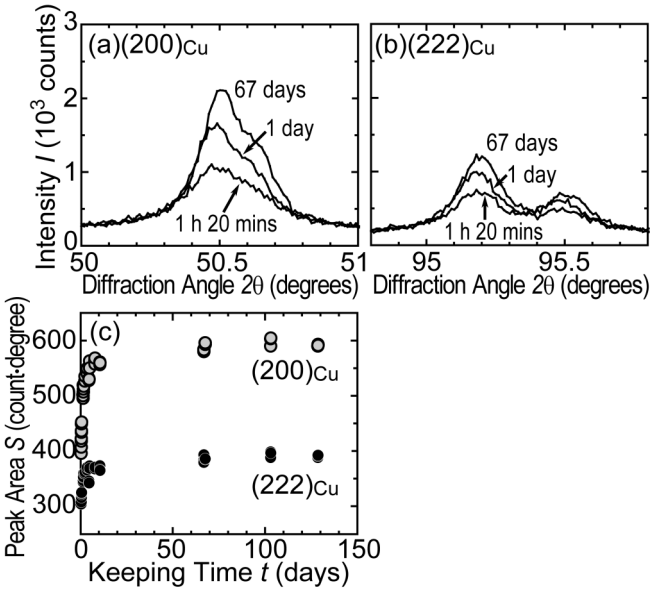

Fig. 1

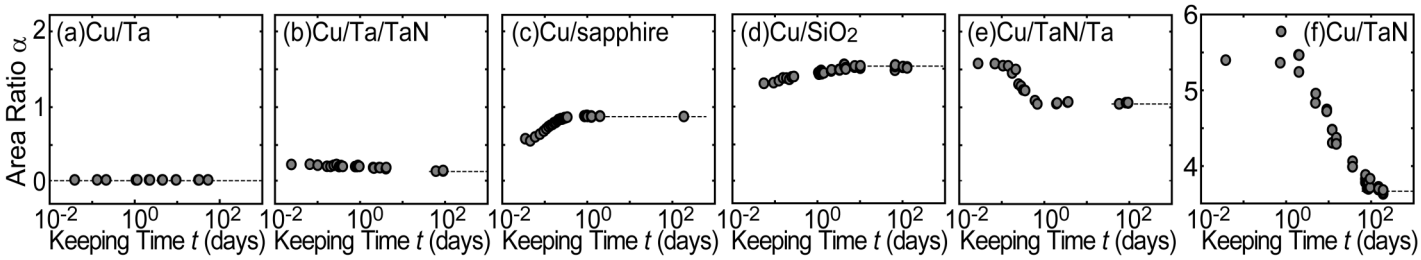

Fig. 2

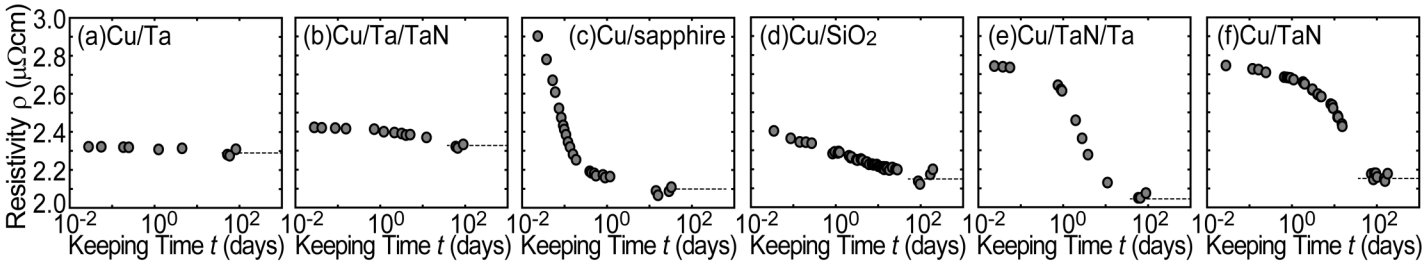

Fig. 3

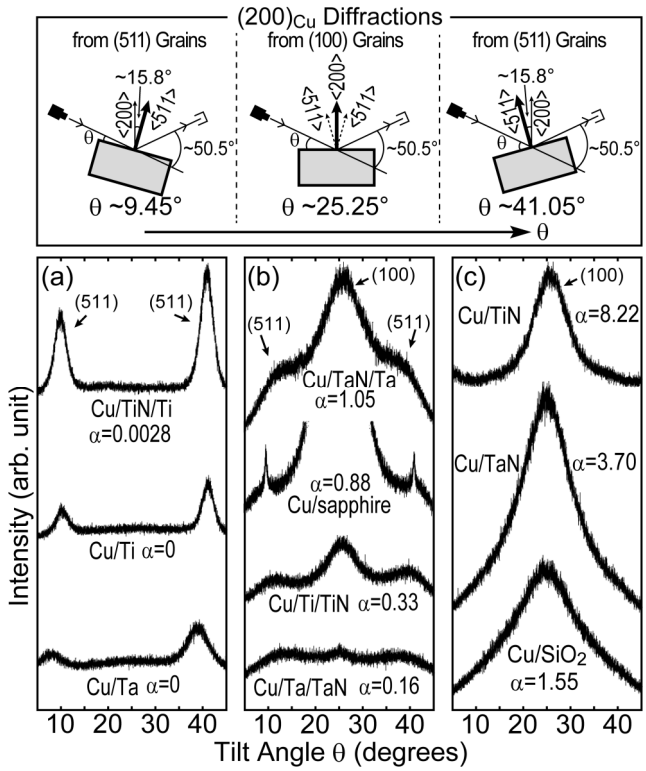
(200)Cu Diffractions
from (511) Grains
from (100) Grains
from (511) Grains
~15.8°
~50.5°
θ ~9.45°
θ ~25.25°
θ ~41.05°
θ
(a)
(b)
(c)
(511)
(100)
Cu/TiN/Ti α=0.0028
Cu/Ti α=0
Cu/Ta α=0
Cu/TaN/Ta α=1.05
α=0.88 Cu/sapphire
Cu/Ti/TiN α=0.33
Cu/Ta/TaN α=0.16
Cu/TiN α=8.22
Cu/TaN α=3.70
Cu/SiO2 α=1.55
Intensity (arb. unit)
10 20 30 40
Tilt Angle θ (degrees)

Fig. 4

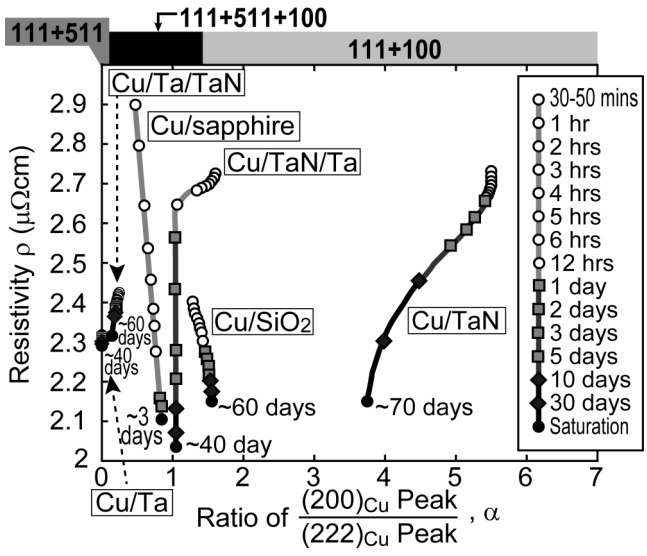
111+511
111+511+100
111+100
Cu/Ta/TaN
Cu/sapphire
Cu/TaN/Ta
Cu/SiO2
Cu/TaN
~60 days
~40 days
~3 days
~40 day
~60 days
~70 days
Cu/Ta
30-50 mins
1 hr
2 hrs
3 hrs
4 hrs
5 hrs
6 hrs
12 hrs
1 day
2 days
3 days
5 days
10 days
30 days
Saturation
Resistivity ρ (μΩcm)
Ratio of (200)Cu Peak / (222)Cu Peak , α

Fig. 5

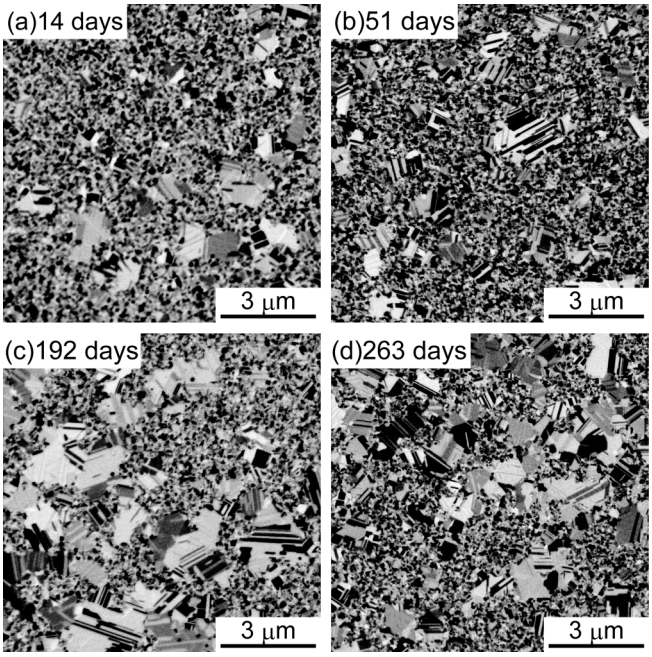

Fig. 6

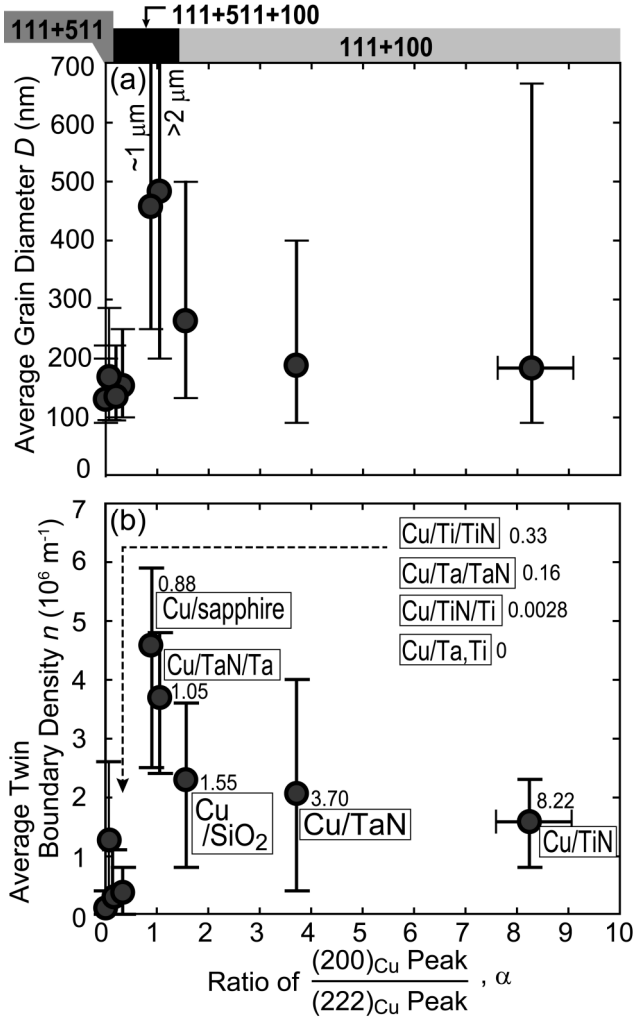
111+511
111+511+100
111+100
(a)
~1 μm
>2 μm
Average Grain Diameter D (nm)
(b)
Cu/Ti/TiN 0.33
Cu/Ta/TaN 0.16
Cu/TiN/Ti 0.0028
Cu/Ta,Ti 0
0.88
Cu/sapphire
Cu/TaN/Ta
1.05
1.55
Cu /SiO2
3.70
Cu/TaN
8.22
Cu/TiN
Average Twin Boundary Density n (10^6 m^-1)
Ratio of (200)Cu Peak / (222)Cu Peak , α

Fig. 7

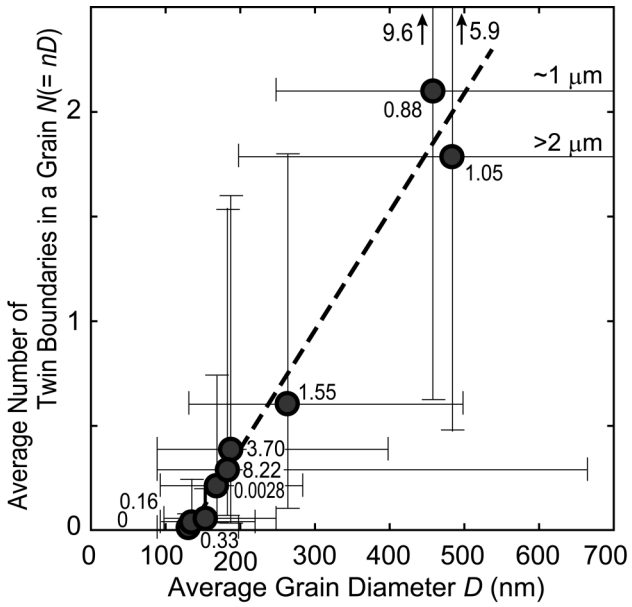
9.6
5.9
~1 μm
0.88
>2 μm
1.05
1.55
3.70
8.22
0.0028
0.16
0
0.33
Average Number of
Twin Boundaries in a Grain N(= nD)
Average Grain Diameter D (nm)
0
1
2
0
100
200
300
400
500
600
700

Fig. 8

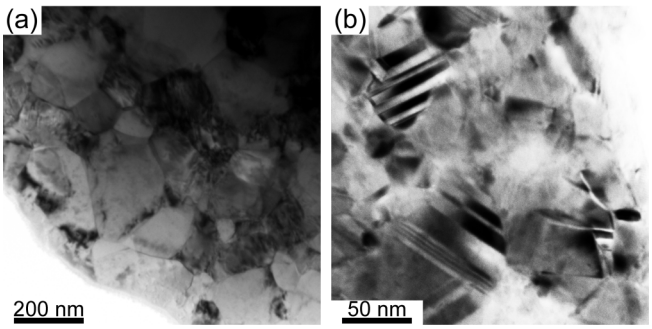
(a)
200 nm
(b)
50 nm

Fig. 9

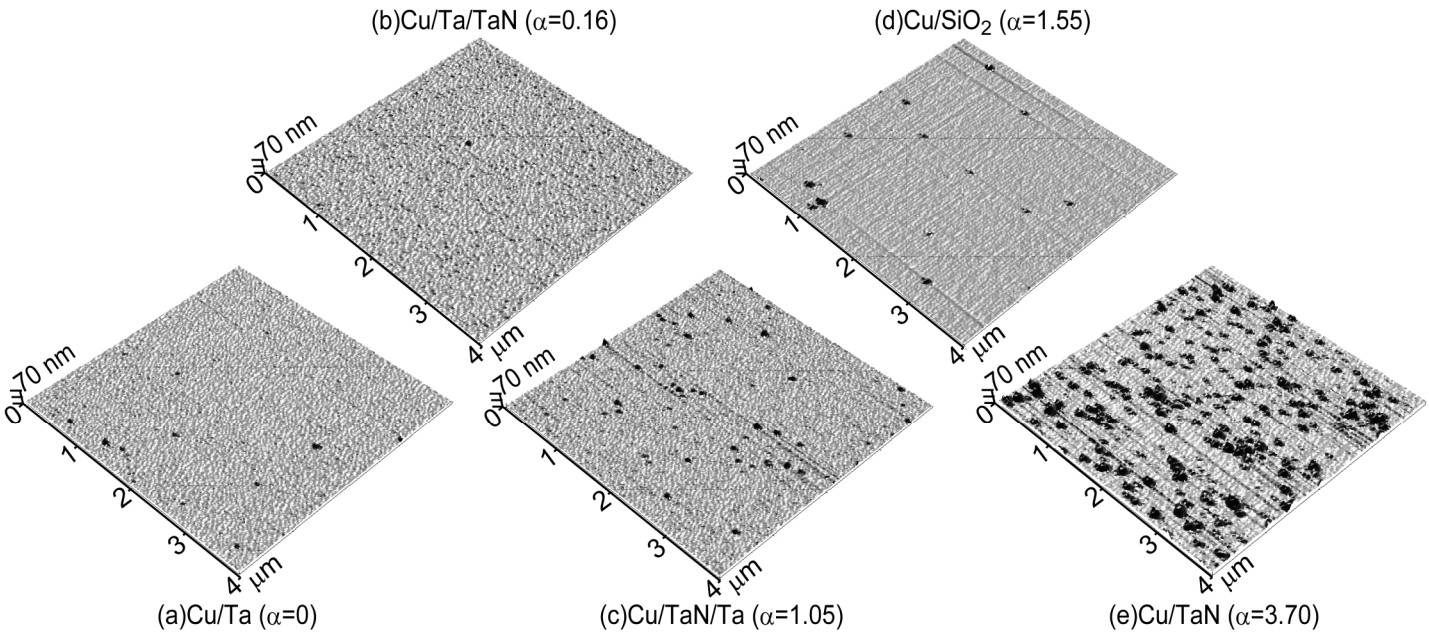
(b)Cu/Ta/TaN (α=0.16)
(d)Cu/SiO2 (α=1.55)
70 nm
0
1
2
3
4 μm
(a)Cu/Ta (α=0)
(c)Cu/TaN/Ta (α=1.05)
(e)Cu/TaN (α=3.70)

Fig. 10

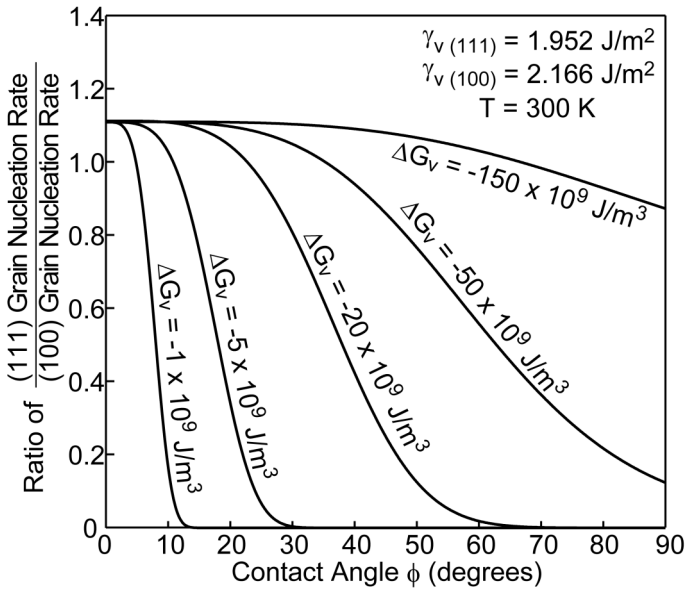
γv (111) = 1.952 J/m2
γv (100) = 2.166 J/m2
T = 300 K
ΔGv = -150 x 10^9 J/m3
ΔGv = -50 x 10^9 J/m3
ΔGv = -20 x 10^9 J/m3
ΔGv = -5 x 10^9 J/m3
ΔGv = -1 x 10^9 J/m3
Ratio of (111) Grain Nucleation Rate / (100) Grain Nucleation Rate
Contact Angle ϕ (degrees)
0
0.2
0.4
0.6
0.8
1.0
1.2
1.4
10
20
30
40
50
60
70
80
90

Fig. 11